Permanent Magnet Shape Optimization Method for PMSM Air Gap Flux Density Harmonics Reduction

Chengsi Liu, Yongxiang Xu, *Member, IEEE,* Jibin Zou, *Senior member, IEEE,* Guodong Yu, *Member, IEEE,* and Liang Zhuo

***Abstract*—This paper proposed a permanent magnet optimization method to suppress the air gap flux density harmonic of permanent magnet synchronous motor (PMSM). The method corrected the effective air gap length of the motor, calculated the magnetization length of the permanent in the case of parallel magnetization, and took the influence of the permanent magnet relative permeability into consideration. Based on these works, for a given sinusoidal air gap flux density waveform, the corresponding structural parameters can be calculated, so as to achieve the optimization of the permanent magnet. By using this method to optimize the shape of the magnet, the fundamental wave of the air gap flux density can be retained to the greatest extent, so as to eliminate harmonics and maintain the output capacity at the same time. The feasibility and accuracy of the method have been verified by finite element analysis (FEA) and prototype machine experiment. This method is simple and time-saving, and has a satisfactory accuracy, which provides a reference method for permanent magnet optimization of PMSM.**

***Index Terms*—Permanent magnet synchronous motor (PMSM), analytical method, finite element analysis (FEA), magnet shape optimization.**

I. Introduction

PERMANENT magnet synchronous motor (PMSM) is widely used in industrial production because of the advantages of simple structure, high power density, high efficiency and smooth operation [1],[2]. The electromagnetic performance of PMSM, such as the cogging torque, the electromagnetic torque, the torque ripple, the noise and the vibration, is related to the waveform of the air gap flux density. Reducing the air gap flux density harmonics can effectively mitigate the cogging torque, suppress the torque ripple, and decrease the noise and vibration level of the machine, so as to ensure the smooth operation of the PMSM and realize high quality motor control performance [3]-[5]. Therefore, it's of great significance to find an optimal design method that can make the air gap flux density sinusoidal.

The harmonics of PMSM air gap flux density can be reduced by both motor design and control strategy [6]-[10]. In terms of PMSM design, permanent magnet optimization is one of the most effective and commonly used methods [11]. By optimizing the structural parameters of the permanent magnet, the harmonics of the air gap flux density can be reduced so as to obtain a sinusoidal air gap flux density [12,13]. The main permanent magnet shape optimization methods include sinusoidal shaping optimization, inverse cosine shaping optimization and eccentric optimization. The sinusoidal shaping optimization is to optimize the magnetization thickness of permanent magnet $\Delta h(\theta)$ according to the sinusoidal function of rotor position angle θ, so as to obtain a sinusoidal air gap flux density waveform [14]-[16]. And the inverse cosine shaping optimization is to optimize the air gap length $l_g(\theta)$ according to the inverse cosine function of rotor position θ [17]-[19]. The schematic diagram of sinusoidal shaping method and inverse cosine shaping method is shown as Fig.1. It should be noticed that both sinusoidal and inverse cosine shaping optimization method are proposed for radial magnetization. But for the widely used parallel magnetized permanent magnet, the optimization results of the two methods are not ideal. Another commonly used permanent magnet optimization method is eccentric optimization. This method is to optimize the inner and outer arcs of the permanent magnet from traditional concentric arcs to eccentric state, so as to reduce the air gap flux density harmonics to obtain sinusoidal flux density [20]-[23]. The schematic diagram of the eccentric optimization is shown as Fig.2. It should be noticed that the eccentric optimization has only one variable of eccentricity h, so it's difficult to balance the sinusoidal degree and amplitude of the air gap flux density, which may decrease the output capacity of the PMSM.

The existing permanent magnet optimization methods are mostly for radial magnetization and give less consideration to the maintenance of air gap flux density amplitude when reducing harmonics. To solve these problems, this paper proposed an analytical optimization method. The method

Manuscript received October 09, 2021; revised November 05, 2021; accepted November 16, 2021. date of publication December 25, 2021; date of current version December 18, 2021.

Chengsi Liu and Guodong Yu are with School of Electrical Engineering and Automation of HIT.(e-mail: liuchengsi1994@live.com; yuguodong@hit.edu.cn

Yongxiang Xu is with Department of Electrical Engineering, Harbin Institute of Technology.(e-mail: xuyx@hit.edu.cn)

Jibin Zou is with the State Key Laboratory of Robotics and System, Harbin Institute of Technology.(e-mail: zoujibin@hit.edu.cn)

Liang Zhuo is with Harbin Institute of Technology and National Engineering Research Center for Small and Special Precision Motors, Guizhou Aerospace Linquan Motor Co. Ltd.(e-mail: zhuolianghit@163.com)

(Corresponding Author: Chengsi Liu)

Digital Object Identifier 10.30941/CESTEMS.2021.00033

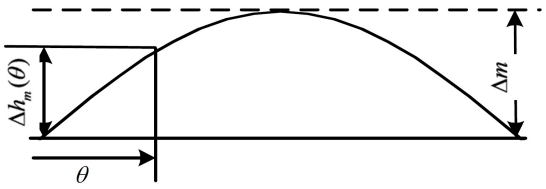

(a) Sinusoidal shaping optimization

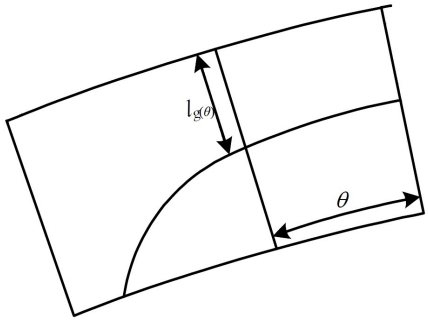

(b) Inverse cosine shaping optimization

Fig. 1. Illustration of sinusoidal shaping optimization and inverse cosine shaping optimization of surface mounted permanent magnet.

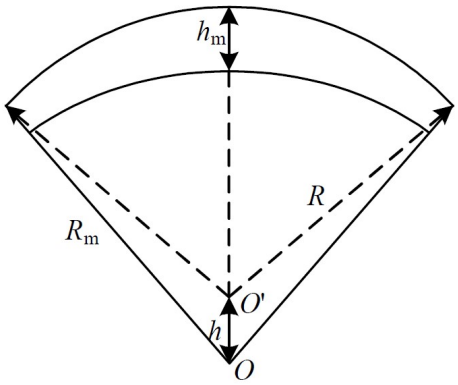

Fig. 2. Illustration of eccentric optimization of surface mounted permanent magnet.

corrected the effective air gap length of the motor, calculated the magnetization length of the permanent in the case of parallel magnetization, and took the influence of the permanent magnet relative permeability into consideration. Based on these works, a more accurate relationship between air gap flux density and relevant structure parameters can be obtained and expressed as a calculation formula. According to the formula, for a given sinusoidal air gap flux density waveform, the corresponding structural parameters can be calculated, so as to achieve the optimization of the permanent magnet. The output capacity can be maintained by giving a sinusoidal air gap flux density with a large amplitude. Finite elements analysis (FEA) is taken to calculate the electromagnetic performance of the PMSM before and after optimization, and a 1.8 kW prototype is made and experimented to verify the feasibility and accuracy of the method.

II. Proposed Method

Because of the symmetry of magnetic poles of PMSM, half of a single permanent magnet of PMSM can be selected for modeling. The model is shown as Fig.3, where the positive direction of y axis is the magnetization direction, R_s is the inner radius of the stator, R_i is the inner radius of the permanent magnet, θ_1 and θ_2 are the rotor position angle, α is the position angle of the side of the permanent magnet, $\Delta R(\theta_2)$ is the radial distance between inner radius and outer radius of permanent magnet at the position angle θ_2, $\Delta h(\theta_2)$ is the magnetization length at the position angle θ_2, and the $l_g(\theta_2)$ is the length of the gap at position angle θ_2.

α can be expressed as:

$$\alpha = \frac{\pi}{2} - \frac{\pi}{2p} \tag{1}$$

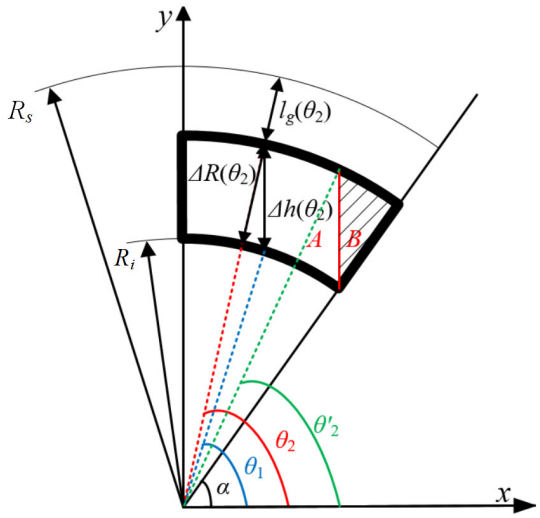

Fig. 3. The model of the half of a single permanent magnet.

where p is the pole pairs of the PMSM.

The magnet can be separated into two parts A and B. The boundary of the two parts is

$$x = R_i \cos\alpha \tag{2}$$

The boundary position angle is

$$\theta_2^{'} = \arccos\frac{R_i \cos\alpha}{R_i + \Delta R(\theta_{2'})} \tag{3}$$

$\Delta h(\theta_2)$ is the magnetization length at the position angle θ_2, which can be described as

$$\Delta h(\theta_2) = \begin{cases} [R_i + \Delta R(\theta_2)]\sin\theta_2 - R_i \sin\theta_1 & , \theta_2 \in \left[\theta_2^{'}, \frac{\pi}{2}\right] \\ [R_i + \Delta R(\theta_2)]\sin\theta_2 - \\ [R_i + \Delta R(\theta_2)]\cos\theta_2 \tan\alpha & , \theta_2 \in \left[\alpha, \theta_2^{'}\right) \end{cases} \tag{4}$$

The relationship between θ_1 and θ_2 is

$$[R_i + \Delta R(\theta_2)]\cos\theta_2 = R_i \cos\theta_1 \tag{5}$$

So the formula (4) can be further expressed as:

$$\Delta h(\theta_2) = \begin{cases} [R_i + \Delta R(\theta_2)]\sin\theta_2 - \\ R_i \sin[\arccos(\frac{[R_i + \Delta R(\theta_2)]\cos\theta_2}{R_i})] & , \theta_2 \in \left[\theta_2^{'}, \frac{\pi}{2}\right] \\ [R_i + \Delta R(\theta_2)]\sin\theta_2 - \\ [R_i + \Delta R(\theta_2)]\cos\theta_2 \tan\alpha & , \theta_2 \in \left[\alpha, \theta_2^{'}\right) \end{cases} \tag{6}$$

The air gap length can be expressed as:

$$l_g(\theta_2) = R_s - R_i - \Delta R(\theta_2) \tag{7}$$

For the convenience of calculation, the relative permeability of the core is regarded as infinite, so only the effect of air gap reluctance on air gap flux density needs to be considered. The radial air gap flux density $B_g(\theta_2)$ can be expressed as:

$$B_g(\theta_2) = \frac{B_r \Delta h(\theta_2) \sin\theta_2}{\Delta h(\theta_2) + \mu_r l_g(\theta_2) \sin\theta_2} \tag{8}$$

where B_r is the remanence of the permanent magnet, and μ_r is the relative permeability of the permanent magnet.

$$B_g(\theta_2) = \begin{cases} \dfrac{B_r \sin\theta_2}{1 + \dfrac{\mu_r [R_s - R_i - \Delta R(\theta_2)] \sin\theta_2}{[R_i + \Delta R(\theta_2)] \sin\theta_2 - R_i \sin\left\{\arccos\left[\dfrac{R_i \cos\theta_2 + \Delta R(\theta_2)\cos\theta_2}{R_i}\right]\right\}}}, & \theta_2 \in \left[\theta_2', \dfrac{\pi}{2}\right] \\ \dfrac{B_r \sin\theta_2}{1 + \dfrac{\mu_r [R_s - R_i - \Delta R(\theta_2)] \sin\theta_2}{[R_i + \Delta R(\theta_2)] \sin\theta_2 - [R_i + \Delta R(\theta_2)] \cos\theta_2 \tan\alpha}}, & \theta_2 \in \left[\alpha, \theta_2'\right) \end{cases} \tag{9}$$

Combined with formula (6) and (7), formula (8) can be further expressed as:

It can be seen from (9) that $B_g(\theta_2)$ is related to variables $\Delta R(\theta_2)$ and θ_2. When giving a certain $\Delta R(\theta_2)$, the $B_g(\theta_2)$ can be calculated by formula (9). And because of the corresponding relationship, when giving a certain $B_g(\theta_2)$, the $\Delta R(\theta_2)$ can be also obtained by calculating inverse solution of formula (9). It can be known from Fig.3 that the range of the whole magnet pole is from α to π-α in mechanical degree, and the corresponding electrical degree range is from 0° to π. The target radial flux density during the range should be a standard sinusoidal wave of half a cycle, so the $B_g(\theta_2)$ can be expressed as (10). By combining formula (9) and (10), the optimization parameters $\Delta R(\theta_2)$ can be calculated.

$$B_g(\theta_2) = B_{amp} \sin\left[\frac{(\theta_2 - \alpha)\pi}{\pi - 2\alpha}\right] \tag{10}$$

where B_{amp} is the amplitude of B_g.

B_{amp} should be given as large as possible within the range to ensure the output capacity of the motor, and the specific value of the B_{amp} is determined according to the non-optimized air gap flux density waveform.

III. Analytical Calculation and FEA Verification

A. Initial Model of PMSM

A 9-slot 6-pole surface mounted PMSM is employed to demonstrate the accuracy of the proposed method. The specifications and design parameters are listed in Table I. According to the relevant design parameters, the initial FEA model of the motor can be built shown as Fig.4.

The initial model has not been optimized, so the inner and outer diameters of the permanent magnet are concentric arcs. For the initial model, it is obvious that $\Delta R(\theta_2)$ is a constant, that is, the maximum thickness of the permanent magnet. The analytical solution of air gap flux density can be obtained by formula (9).

The FEA model shown in Fig.4 is employed to calculate the electromagnetic performance under no-load working condition. The air gap flux density waveform can be obtained as shown in Fig. 5.

As can be seen from Fig.5, although the FEA air gap flux density is distorted because of the slots, the two waveforms are still similar. It shows that the analytical results are consistent with EFA results, which proves the accuracy of the proposed method.

TABLE I
Specifications and Design Parameters of the Machine Prototype

Quantity	Value	Unit
Rated Power	1.5	kW
Rated Speed	7500	r/min
Rated Torque	1.9	Nm
Pole pairs	3	-
Number of slots	9	-
Maximum thickness of magnet	3.95	mm
Stator outer diameter	53	mm
Stator inner diameter	26	mm
Rotor outer diameter	23.9	mm
Axial length	72	mm
Relative permeability of magnet	1.05	-
Remanence of magnet	1.3	T

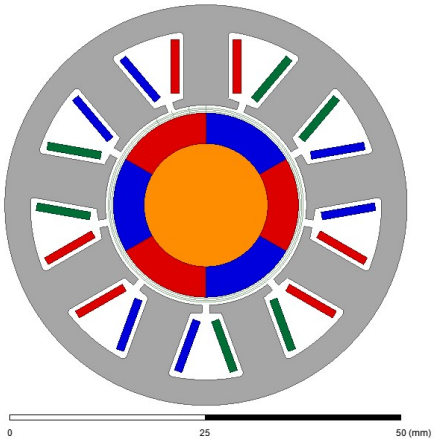

Fig. 4. Initial FEA model of the 9-slot 6-pole PMSM

B. Extracting Sinusoidal Flux Density with Maximum Amplitude

Based on the analytical air gap flux density waveform, the sinusoidal air gap flux density as the optimization target can be extracted. The value of the analytical air gap flux density at the electrical angle of 90° should be selected as the amplitude of

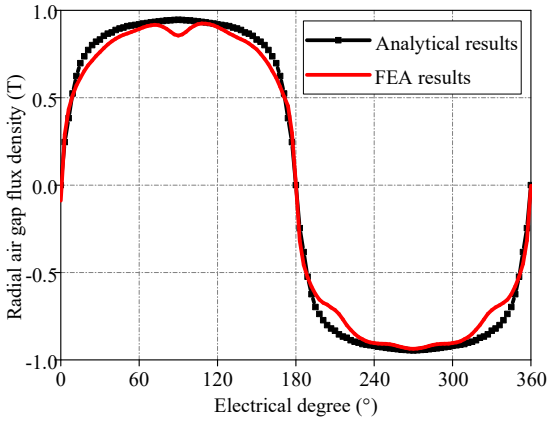

Fig. 5. Comparison of analytical and FEA radial air gap flux density.

the target air gap flux density, so as to ensure the obtained air gap flux density has the maximum amplitude to retain the output capacity of the PMSM. The analytical air gap flux density and the target sinusoidal air gap flux density are shown in Fig. 6.

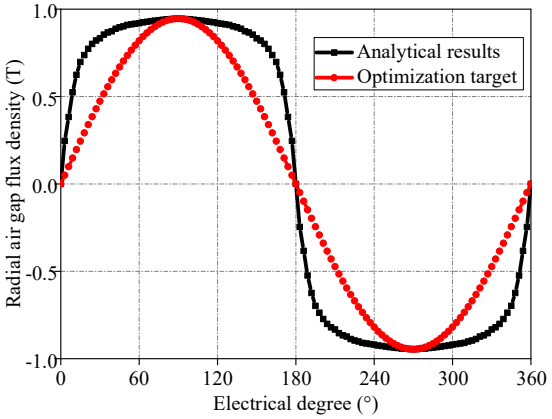

Fig. 6. Analytical radial air gap flux density and the target radial air gap flux density.

Fast Fourier Transformer (FFT) results of the analytical and the target air gap flux density are shown in Fig.7. It should be noticed that although the target air gap flux density has the same maximum value with the non-optimized one, it has a lower fundamental amplitude. In addition, harmonics are all eliminated, so the output capacity of the motor will decrease after optimization.

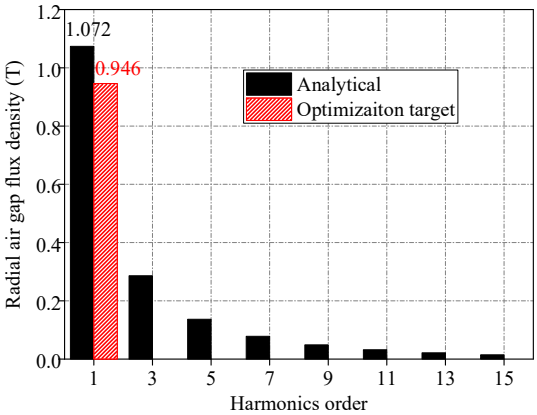

Fig. 7. FFT results of analytical radial air gap flux density and the target radial air gap flux density.

Although the decrease is unavoidable, the output capacity of the motor can be retained as much as possible by selecting a large fundamental amplitude of target air gap flux density as shown in Fig.6.

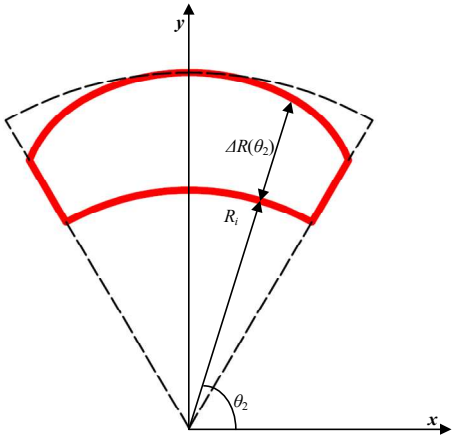

Fig. 8. Illustration of optimized permanent magnet.

C. Optimized Model of PMSM

Taking optimization target air gap flux density shown in Fig.6 as $B_g(\theta_2)$, formula (9) can be used to calculate the optimization parameter $\Delta R(\theta_2)$. Based on the results of $\Delta R(\theta_2)$, the permanent magnet can be optimized as shown in Fig.8.

Then the model of PMSM using the optimized permanent magnet is shown in Fig. 9.

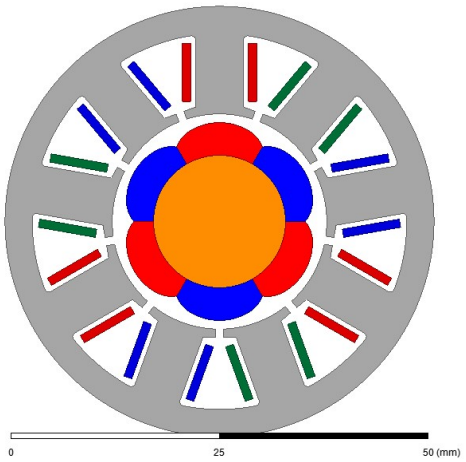

Fig. 9. Optimized model of 9-slot 6-pole PMSM.

The FEA model shown in Fig.9 is employed to calculate the electromagnetic performance under no-load working condition. The air gap flux density waveform can be obtained as shown in Fig.10. Compared with the target air gap flux density, the FEA air gap flux density has a smaller amplitude. This is because the reluctance of the core is ignored in analytical calculation. And it can be seen from Fig.10 that although the FEA air gap flux density is distorted because of the slots, the waveform is similar to the sinusoidal target air gap flux density.

D. Comparison of Initial and Optimized Model

The initial model and the optimized model are employed respectively to calculate the electromagnetic performance of the PMSM under no-load and load working conditions, and the results are compared.

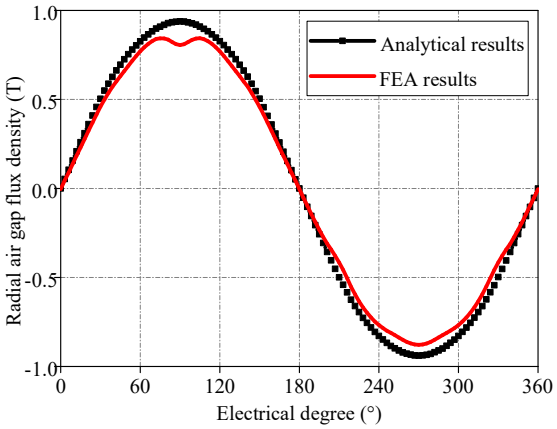

Fig. 10. Comparison of analytical and FEA radial air gap flux density.

The line back EMF of the two models are calculated under no-load condition and shown as Fig.11. The maximum of the two waveforms are 92.553V and 78.1738V while the effective values are 62.1V and 55.64V.

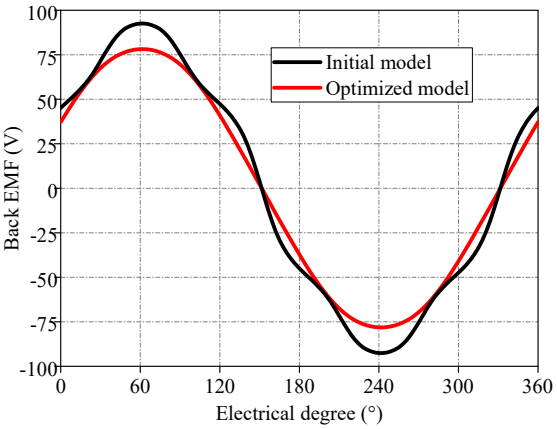

Fig. 11. Comparison of line back EMF of initial and optimized model.

Compared with the distorted flux density waveform, the back EMF waveforms can reflect the harmonics of the air gap flux density without being affected by slotting. FFT is performed to the back EMF waveforms, and the results are shown as Fig.11. It can be seen from Fig.11 that the optimized model effectively suppresses the back EMF harmonics. By optimizing the permanent magnet, the fundamental amplitude of the back EMF is reduced from 89V to 78.7V, while the total harmonics distortion is reduced from 7.5% to 0.61%.

As an important index affecting the stable operation, the cogging torque is also calculated by the initial and optimized model under the no-load working condition as shown in Fig.13. The amplitude of the cogging torque is reduced from 140 mNm to 12 mNm sharply.

Three-phase sinusoidal current is applied to the initial and optimized FEA models to calculate the rated torque, and the results are shown as Fig.14. By optimizing the permanent magnet, the amplitude of the torque ripple is reduced from 210 mNm to 40 mNm.

According to the above electromagnetic performance calculations, it's proved that the optimization method proposed by this paper can effectively suppress the harmonics of back EMF, decrease the cogging torque and torque ripple, so as to ensure the smooth operation of the motor.

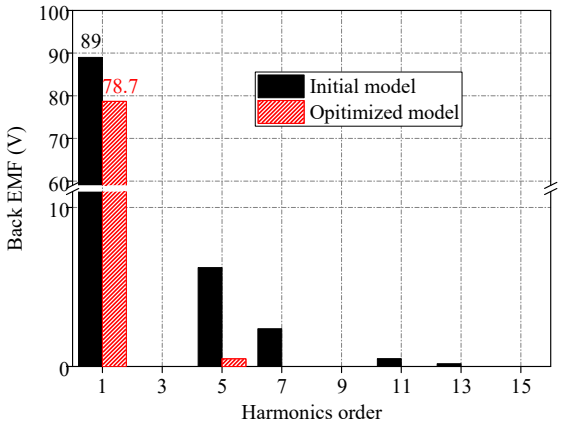

Fig. 12. FFT results of line back EMF of initial and optimized model.

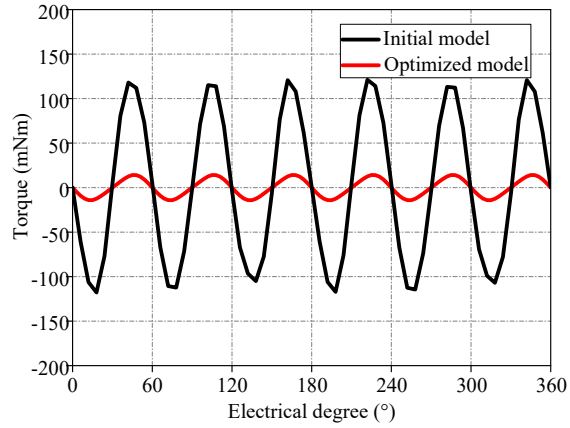

Fig. 13. Comparison of cogging torques of initial and optimized model.

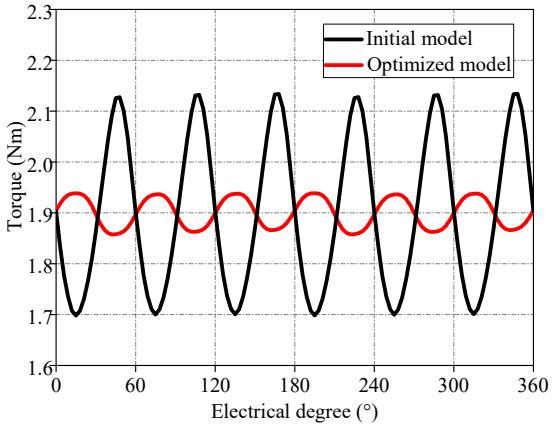

Fig. 14. Comparison of electromagnetic torque of initial and optimized model.

IV. Experimental Vlidation

A. Prototype Machine

A prototype machine is made based on the optimized permanent magnet shape. The permanent magnet and the prototype machine are shown as Fig.15.

B. Experimental Results

Because the air gap flux density is difficult to measure directly, the line back EMF waveform is selected as the measurement object. The prototype machine is tested under no-load working condition, and the line back EMF is measured and compared with the FEA results as shown in Fig.16. It can

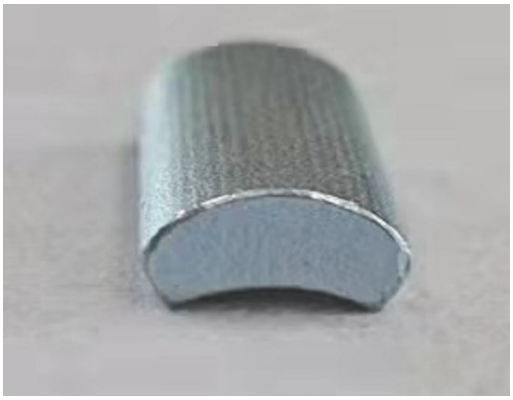

(a) Optimized permanent magnet

(b) Prototype machine

Fig. 15. Prototype machine of 1.5 kW 9-slot 6-pole PMSM

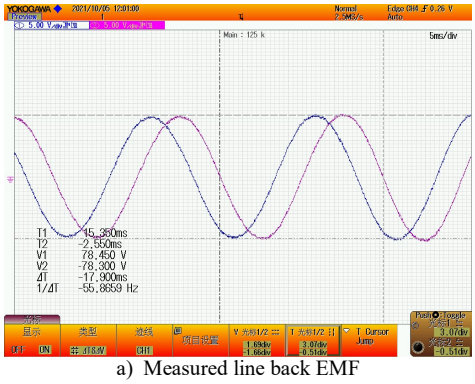

a) Measured line back EMF

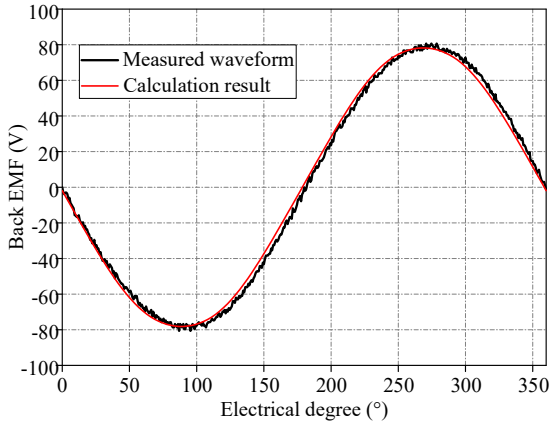

b) Compared with the FEA result.

Fig. 16. Experimental result of line back EMF of the optimized PMSM.

be seen from Fig. 16 that the measured waveform dovetails with the FEA results well.

FFT analysis is performed to the measured line back EMF waveform. The Total Harmonics Distortion (THD) of the measured line back EMF waveform is 0.76%, which is consistent with the calculation result of 0.61%. The small value of the THD indicates that the measured line back EMF waveform is highly sinusoidal, which proves the air gap flux density is highly sinusoidal, thus proving the accuracy of the proposed magnet optimization method.

V. Conclusion

This paper proposed a permanent magnet optimization method which can suppress the air gap flux density harmonics. In this paper, the relationship between air gap flux density and parameters in parallel magnetization is given. Based on the inverse solution of the expression, the structural parameters of permanent magnet corresponding to the sinusoidal air gap flux density can be obtained, so as to achieve the optimization of the motor. The accuracy of this method is verified by FEA calculation and experiment. This method is simple and timesaving, and has a satisfactory accuracy, which provides a reference method for permanent magnet optimization of PMSM.

References

[1] D. Staton, A. Boglietti and A. Cavagnino. “Solving the More Difficult Aspects of Electric Motor Thermal Analysis in Small and Medium Size Industrial Induction Motors,” *IEEE Trans. Energy Convers*, vol. 20, no. 3, pp. 620-628, 2005.

[2] X. Cai, M. Cheng, S. Zhu and J. Zhang, "Thermal Modeling of Flux-Switching Permanent-Magnet Machines Considering Anisotropic Conductivity and Thermal Contact Resistance," *IEEE Trans. Ind. Electron*, vol. 63, no. 6, pp. 3355-3365, 2016.

[3] K. Wang, Z. Q. Zhu, G. Ombach, and W. Chlebosz, “Optimal rotor shape with third harmonic for maximizing torque and minimizing torque ripple in IPM motors,” *IEEE Trans. Ind. Electron*, vol. 8, no. 12, pp. 397-403, 2012.

[4] C. L. Xia, Z. Zhang and Q. Geng. “Analytical modeling and analysis of surface mounted permanent magnet machines with skewed slots” *IEEE Trans. Magn*, vol. 51, no. 5, pp. 1-8, 2015.

[5] K. Wang, Z. Q. Zhu, G. Ombach, et al, “Average Torque Improvement of Interior Permanent-Magnet Machine Using Third Harmonic in Rotor Shape,” *IEEE Trans. Ind. Electron*, vol. 61, no. 9, pp. 5047-5057, 2012.

[6] S. Chaithongsuk, N. Takorabet, and F. Meibody-Tabar. “On the use of pulse width modulation method for the elimination of flux densityharmonics in the air-gap of surface PM motors,” *IEEE Trans. Magn*, vol. 45, no. 3, pp. 1736-1739, 2010.

[7] J. Liang, X. F. Zhang and M. Z. Qiao, “On the use of pulse width modulation method for the elimination of flux densityharmonics in the air-gap of surface PM motors,” *IEEE Trans. Magn*, vol. 49, no. 7, pp. 5742-5748, 2013.

[8] P. F. Hu, D. Wang, S. B. Jin, et al. “Sinusoidal Optimization Model for Air Gap Magnetic Field of Eccentric Magnetic Pole Permanent Magnet Motor”, *Transactions of China Electrotechnical Society*, vol. 34, no. 18, pp 3759-3768, 2019.

[9] K.Wang, H. Sun, L. F. Zhang, et al. “An Overview of Rotor Pole Optimization Techniques for Permanent Magnet Synchronous Machines” *Proceedings of the CSEE*, vol. 37, no.24, pp7304-7317.

[10] M. S. Islam, S. Mir, T. Sebastian, and S. Underwood, "Design considerations of sinusoidally excited permanent-magnet machines for low-torque ripple applications," *IEEE Trans. Ind. Appl*., vol. 41, no. 4, pp. 955–962,

[11] Y. B. Yang, X. H. Wang, and C. Q. Zhu. "Effect of permanent magnet segmentation on the cogging torque of surface mounted permanent magnet motors". *Transactions of China Electrotechnical Society*, vol. 27, no.3, pp. 73-78, 2012

[12] B. Y. Zhang, Y. Q. Jia, K. Li, et al. "Study on magnetic pole structure of surface mounted PMSM". *Electric Machines and Control*, vol. 18, no. 5, pp. 43-48, 2014

[13] Y. Li, J. B. Zou and Y. P. Lu. "Optimum design of magnet shape in permanent-magnet synchronous motors". *IEEE Trans. Magn*, vol. 39, no. 6, pp. 3523-3526, 2003.

[14] K. Wang, Z. Q. Zhu and G. Ombach. "Torque enhancement of surface-mounted permanent magnet machine using third-order harmonic" *IEEE Trans. Magn*, vol. 50, no. 3, 2014.

[15] S. Ruangsinchaiwanich, Z. Q. Zhu and D. Howe. "D. Influence of magnet shape on cogging torque and back-EMF waveform in permanent magnet machines". *International Conference on Electrical Machines and Systems*. Nanjing, China: IEEE, 2005: 284-289.

[16] F. Chai, P. Liang, Y. Pei, et al. "al. Magnet shape optimization of surface-mounted permanent-magnet motors to reduce harmonic iron losses". *IEEE Trans. Magn*, vol. 52, no. 7, pp. 1-4, 2016.

[17] M. F. Hsieh, S. Y. Hsu. "An investigation on influence of magnet arc shaping upon back electromotive force waveforms for design of permanent-magnet brushless motors". *IEEE Trans. Magn*, vol. 41, no. 10, pp. 3949-3951, 2005.

[18] Z. Chen, C. Xia, Q. Geng, et al. "Modeling and analyzing of surface-mounted permanent-magnet synchronous machines with optimized magnetic pole shape". *IEEE Trans. Magn*, vol.50, no. 11, pp. 1-4, 2014.

[19] P. Zheng, Z. Lin and Y. Sui. "Research on combined pole for interior permanent-magnet machine". *IEEE International Magnetics Conference*. Beijing, China: IEEE, 2015: 1.

[20] H. J. Liang, X. F. Zhang, m. z. Qiao, et al. "Optimal design and multifield coupling analysis of propelling motor used in a novel integrated motor propeller". *IEEE Trans. Magn*, vol. 49, no. 7, pp. 5742-5748, 2013.

[21] Y. Zhou, H. S. Li and G. W. Meng. "Analytical calculation of magnetic field and cogging torque in surface-mounted permanent-magnet machines accounting for any eccentric rotor shape". *IEEE Trans. Ind. Electron*, vol. 62, no. 6, pp. 3438-3447, 2015.

[22] Y. Zhou, H. S. Li and N. N. Ren. "Analytical calculation and optimization of magnetic field in spoke-type permanent-magnet machines accounting for eccentric pole-arc shape". *IEEE Trans. Magn*, vol. 53, no. 9, pp.1-7, 2013.

[23] Y. Duan, D. M. Inoel. "A review of recent developments in electrical machine design optimization methods with a permanent magnet synchronous motor benchmark study". *IEEE Trans. Magn*, vol. 49, no. 3, pp.1268-1275, 2013.

Chengsi Liu was born in Shaanxi Province, China, in 1994. He received the B.S. and M.S. degrees in electrical engineering from the Harbin Institute of Technology (HIT), Harbin, China, in 2016 and 2018, respectively. He is currently pursuing the Ph.D. degree in School of Electrical Engineering and Automation of HIT.

His current research interests include permanent magnet motor design and optimization.

Yongxiang Xu (M'03) received his M.S. and Ph.D. degrees in electrical engineering from the Harbin Institute of Technology, Harbin, China, in 2001 and 2005, respectively.

In 2005, he joined the Department of Electrical Engineering, Harbin Institute of Technology as an assistant professor. Since 2013, he has been a professor in the Department of Electrical Engineering, Harbin Institute of Technology. His current research interests include permanent-magnet machine design and control.

Jibin Zou (SM'00) received the M.S. and Ph.D. degrees in electrical engineering from the Harbin Institute of Technology, Harbin, China, in 1984 and 1988, respectively.

Since 1985, he has been engaged in the research in electrical machines. He was with the University of Liverpool, Liverpool, U.K. as a Visiting Research Fellow for one year. He is now a Professor in the State Key Laboratory of Robotics and System, Harbin Institute of Technology.

Prof. Zou is a senior member of the IEEE Magnetics society, since 2000. His current research interests include permanent-magnet machine design and control.

Guodong Yu (M'20) received the B.Sc. degree in electrical engineering from the Harbin University of Science and Technology, Harbin, China, in 2010, and the M.Sc. and Ph.D. degrees in electrical engineering from the Harbin Institute of Technology (HIT), Harbin, in 2012 and 2017, respectively.

Since 2018, he has been with the School of Electrical Engineering and Automation, HIT. His current research interest includes the design and optimization of permanent magnet machines.

Liang Zhuo was born in Zhangjiajie, China in 1986. He received the M.S. degree in electrical engineering from Guangdong University of Technology, Guangzhou, China, in 2012. He is currently pursuing his Ph.D. degree in electrical engineering from Harbin Institute of Technology.

He is currently a senior engineer in National Engineering Research Center for Small and Special Precision Motors, Guizhou Aerospace Linquan Motor Co. Ltd. His major research interests include the design, analysis and control of permanent magnet machines, high-reliability permanent magnet synchronous anti-short-circuit generator and low voltage DC starter-generator, etc.